Time-Resolved Probing of Electron Thermal Transport in Plasma Produced by Femtosecond Laser Pulses

B.-T. V. Vu,* A. Szoke, and O. L. Landen
Lawrence Livermore National Laboratory, Livermore, California 94550
(Received 13 December 1993)

We present the first direct evidence for a supersonically moving steep ionization front in a solid density hot plasma. The plasma was produced by irradiating a transparent solid target with 100 fsec laser pulses at a peak intensity of 5×10^{14} W/cm^2. Time-resolved measurements of reflectivity, transmissivity, and frequency shift of a probe light, incident on the rear of the plasma, showed rapid formation of an overdense plasma layer with a steep gradient that penetrates supersonically into the bulk target. Calculations using a simple nonlinear heat wave model, driven by electron thermal transport, show good agreement with the experimental results.

PACS numbers: 52.25.Fi, 52.50.Jm, 52.65.+z, 52.70.Kz

Recent developments in the generation of high power femtosecond laser pulses offer new possibilities in the studies of ultrafast phenomena that were unresolved in the past. One example is the discovery of nonequilibrium electron distributions in metals and semiconductors [1], created by ~100 fsec laser pulses, and the characterization of their relaxation times and their roles in solid-liquid phase transitions [2]. These experiments have been carried out with laser intensities below or near the melting threshold (~10^{12} W/cm^2). Other examples of femtosecond laser spectroscopy include experiments with higher intensities, much above the plasma formation threshold (~10^{13} W/cm^2) [3–6], where high temperature (~10 eV) and solid density plasmas were successfully produced on the surface of a metal, that otherwise can only be found in the interiors of stars or in large-scale laser fusion experiments. In a recent experiment [5], we found that when a transparent solid target is irradiated with a high intensity ultrashort laser pulse, a high temperature and solid density plasma layer is rapidly formed at the target surface by the leading edge of the laser pulse.

On theoretical grounds, it is believed that the energy absorbed at the surface is transported supersonically into the bulk region via electron thermal conduction until expansion of the surface plasma becomes important; this results in a rarefaction wave that competes with the thermal wave [7,8]. The subsequent, quasisteady state of the heated solid is that of the familiar ablative heat wave preceded by a shock wave [9]. In the ablative heat wave regime, hydrodynamics of the plasma is inextricably coupled to thermal transport phenomena. The result is that only complicated computer calculations can predict the outcome of most experiments. Furthermore, while plasma transport and equations of state studies, utilizing ablation driven shock waves, have been carried out with picosecond and nanosecond pulses [10], no experimental evidence for phenomena of thermal transport in the ultrafast heat wave regime has been reported.

In this paper, we report high temporal resolution (~100 fsec) measurements to probe electron thermal transport in a high temperature (~40 eV) solid density plasma produced by pump laser irradiation of a transparent solid target. In addition to probe reflection and transmission measurements, the frequency shifts of the probe pulse are recorded as functions of the relative time delay between the pump and probe pulses, demonstrating the first direct observation of a supersonic thermal wave in solid density hot plasma, as is predicted in the thermal heat wave regime [9]. The frequency shifts of the probe light interacting with the expanding plasma at the front (vacuum-plasma) side determine the plasma ion acoustic velocity and temperature. In contrast, the back (plasma-solid) side probe light, unaffected by hydrodynamic expansion, directly interacts with the bulk region behind the surface. Changes in material properties of the bulk region are a result of energy transport phenomena. Front and back side probing, offering detailed measurements of plasma parameters, provide different but complementary information on the plasma evolution and energy transport mechanisms, and thus verification of the ultrafast thermal transport phenomena. Finally, calculations using a simple nonlinear heat wave model for electron thermal conduction show good agreement with the experimental results.

A detailed schematic of a similar pump and back side probe experiment using 1 psec pulses has been described elsewhere [5,11]. The present laser system [12] includes a colliding pulse, mode locked ring oscillator producing low energy 100 fsec pulses at a center wavelength of $\lambda=616$ nm and a repetition rate of 90 MHz. Pulses are selected for amplification at 10 Hz in a six-pass bowtie amplifier followed by two Bethune amplifiers. The 2 mJ, 100 fsec amplified pulses are then directed into a vacuum spatial filter to improve beam transverse mode quality and focusability, and are split into a strong pump and a weaker probe pulse. The pump pulse is normally incident onto the front surface of a target with a peak intensity of 5×10^{14} W/cm^2 and a focal spot diameter of 75 μm. The back side probe beam arrives at 19° to the normal of the back surface. The probe intensity at a focal spot diameter of 25 μm is 2×10^{10} W/cm^2, sufficiently low to be

0031-9007/94/72(24)/3823(4)$06.00

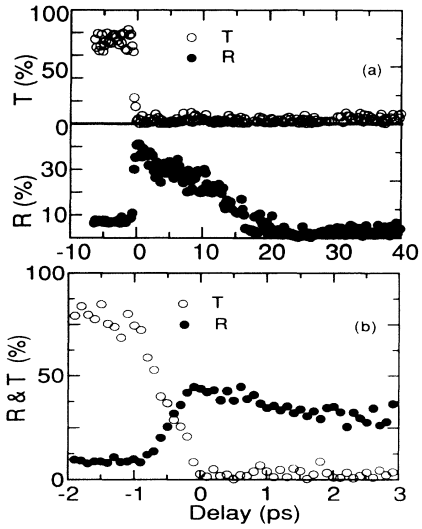

FIG. 1. (a) Single-laser-shot measurements of transmission (open circles) and reflection (closed circles) of a back side probe pulse as functions of delay between the pump and probe pulses. (b) Similar measurements on an expanded time scale.

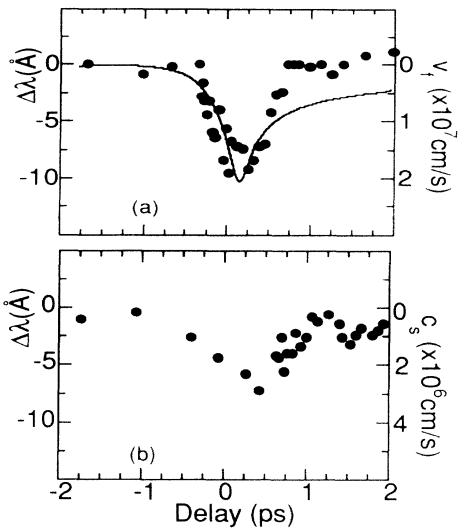

FIG. 2. Measured wavelength shifts (circles) in the reflected (a) back side and (b) front side probe light versus delay. The solid curve is calculated from the nonlinear heat wave model with v_f, the speed of the thermal wave front at the critical density, obtained from Eq. (1). The sound speed c_s is obtained from an isothermal plasma model [14].

nonintrusive but still sufficiently high to discriminate the probe specular reflection from the diffusely scattered light of the intense pump pulse. The probe is S polarized, orthogonal to that of the pump, so that diffusely scattered light of the pump may be more strongly rejected before detection. Energies of the incident, reflected, and transmitted probe are simultaneously monitored by P-I-N photodiodes. In addition to reflectivity and transmissivity measurements, the reflected probe can also be sent to a grating spectrometer (0.33 m, 1200 lines/mm) coupled to a multichannel analyzer (0.4 Å/pixel). The probe beam can also be redirected to probe the plasma from the front side at an angle of 19° to the normal of the front surface. The transparent fused quartz target is 1.6 mm thick and is mounted on a computer-driven translation stage, so that at each shot the laser fires on a fresh part of the target while the overlap conditions of the two beams are well maintained. The target is coated with an antireflection film on its rear surface to suppress probe light reflection from that surface. At the front surface, it is overcoated with an amorphous 300-Å-thick carbon film. The measured cold target absorptivity, reflectivity, and transmissivity are 14.2%, 7.8%, and 78%, respectively. The highly absorptive carbon film promotes large laser absorption and confines laser energy deposition to the surface, thus setting up a high temperature heat source. The film also eliminates induced phase modulation effects [11] and formation of an underdense bulk plasma by the transmitted portion of the pump pulse, by lowering the intensity threshold for critical plasma density formation at the surface [5], hence isolating the effects of thermal transport phenomena.

Figure 1(a) shows simultaneous scans of the back side probe reflection (closed circles) and transmission (open circles) as functions of time delay between the pump and the probe pulses. Zero time delay is estimated to within ± 0.05 psec by comparison with previous experiments [5,11]. Each point is the result of a single laser shot, divided by the incident energy and normalized to the measurements on the cold target. In both data sets, the plateaus during negative delay correspond to the probe arriving earlier and seeing an undisturbed target. When an overdense or supercritical plasma layer is formed at the surface during the onset of the pump pulse, the probe transmission quickly decreases to zero. At the same time, the surface plasma becomes strongly reflective, resulting in an increase in the probe reflection. The large reflection enhancement implies that the plasma, as seen from the rear side in the interior, acts like a mirror, indicating a steep density gradient at suprcritical density and elevated temperatures. At late delay, the reflection increase is followed by a decay with $1/e$ falltime of about 15 psec. This decay is 2.5 times longer than that of the front side probe reflected signals that are decreasing due to plasma expansion [13]. Figure 1(b) shows a similar scan of reflectivity and transmissivity data on an expanded time scale.

In Fig. 2(a) the wavelength shifts $\Delta\lambda$ of the center-of-gravity wavelength component in the spectrum of the reflected back side probe are shown (circles) as a function of delay. Each data point is an average of 90 laser shots and has a statistical uncertainty of ± 0.8 Å. The shifts are assumed to be due to a moving thermal wave or ionization front and are determined by the Doppler formula [14]:

$$\frac{\Delta\lambda}{\lambda} = -2n_s \cos\theta \frac{v_f}{c}. \qquad (1)$$

The factor of 2 accounts for reflection, θ is the incidence angle of the probe, $n_s = 1.46$ is the solid target refractive index, and c and v_f are the speed of light and ionization velocity, respectively. The observed maximum redshift of nearly -10 Å corresponds to a maximum velocity of 1.8×10^7 cm/sec. Figure 2(b) shows the time history of the wavelength shifts in the reflected front side probe light. These shifts are due to combined effects of the motion of the reflecting point and the increase of plasma density in the region in front of it. Estimates of the shifts have been derived using an isothermal plasma expansion model [14]. From the maximum shift of ≈ -7 Å we estimate $c_s = 3.3\times10^6$ cm/sec for the maximum ion acoustic velocity and nearly 40 eV for the maximum temperature of the plasma with an average ionization of 3.5. Hence, the ionization front in the bulk region is supersonic, and it is attributed to a thermal wave created by electron thermal transport. Furthermore, it should be noted that the observed large back side probe shifts and velocities last only for about 1 psec, while the slow decay of the probe reflection indicates the plasma rear surface remains steep and hence specularly reflective for a much longer time (≈ 15 psec).

We now estimate the temperature and electron density evolution in the transparent material by a simple model. The electron temperature profile T_e and density N_e are calculated by the nonlinear heat diffusion equation for electrons (in cgs units unless specified otherwise), assuming no hydrodynamic plasma expansion:

$$\frac{\partial}{\partial t}\left[\frac{3}{2}N_eT_e+\frac{1}{3}\left(2\sum_{z=1}^{8}N_z^{(O)}\chi_z^{(O)}+\sum_{z=1}^{14}N_z^{(Si)}\chi_z^{(Si)}\right)\right]=\frac{\partial}{\partial\chi}\left(k_e\frac{\partial}{\partial\chi}T_e\right). \quad (2)$$

N_z is the density of ions of charge $+z$ and χ_z is the zth ionization energy of the appropriate ion. The first term is the electron thermal energy, and the second and third terms are the energies used for ionization of oxygen and silicon ions, respectively. The right hand side is the electron energy flux. The thermal conductivity for the partially ionized plasma is taken to be Spitzer type [15]: $k_e = 2\times10^{-4}T_e^{5/2}/Z^*$ (erg sec^{-1} K^{-1} cm^{-1}), where Z^* is the average, time dependent ionization of the plasma. N_e and Z^* at a given temperature are calculated by assuming Saha equilibrium [16]; both are $\sim T_e^{3/2}$. The conductivity is thus $\sim T_e$, which scales as that of Lee and More for solid density at temperatures < 30 eV [17].

After the heating ($t > 0$) there is no heat flux at the surface into the surrounding vacuum ($x < 0$). The left boundary condition to the equation is therefore taken to be [18] $T_e(0,t) = T_0e^{2\gamma t}$ during the laser heating ($t \le 0$), and $\partial T_e(0,t)/\partial x = 0$ for $t > 0$. The right boundary condition is $T_e(+\infty,t) = 0$. T_0 is determined by the total absorbed energy. A pump energy absorption of approximately 56% is inferred from the 36% specular reflection and 8% transmission of the pump pulse. The level of scattered light of the pump pulse has been measured by others [3,19] and is small ($< 5\%$) because during the pump pulse there is very little plasma expansion (scale length $L < 100$ Å) and the target surface remains optically flat. In Eq. (2) we have ignored effects of x-ray emission from the plasma because the total Bremsstrahlung emission should account for $< 1\%$ of the plasma energy [20], and the total fluence of blackbody radiation emitted from the surface plasma of 40 eV is negligibly small (0.3 J cm^{-2}) compared to the absorbed pump pulse fluence (25 J cm^{-2}).

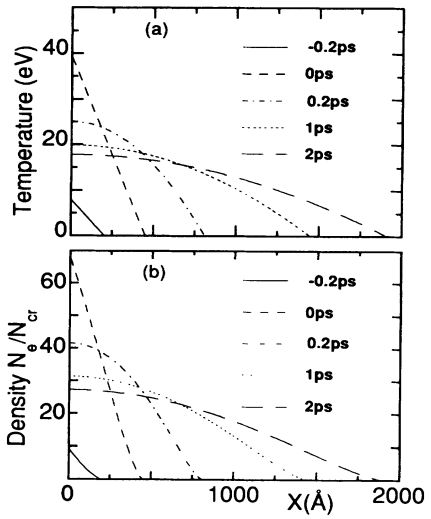

FIG. 3. (a) Calculated electron temperature profiles at different instants as predicted by the nonlinear heat wave model. (b) Corresponding electron density profiles in the bulk target, calculated from the simple approximate solution to the Saha equations [16].

The solution to Eq. (2) for $t < 0$ is similar to that of the Marshak radiation wave [21] and for $t > 0$ the same as that of Zeldovich and Raizer [8]. Figure 3(a) displays calculated snapshots of the temperature profiles at different instants, using $\gamma = 10^{13}$/sec. The surface temperature reaches a maximum of nearly 40 eV, which is in good agreement with the sound speed inferred from the front side probe data [Fig. 2(b)]. At the same time, a thermal wave moves inward supersonically, ionizing the transparent material. For $t > 0$, the surface temperature relaxes gradually and the thermal wave slows down as diffusion of the absorbed energy continues further into the colder region. Figure 3(b) shows the evolution of electron density normalized to the critical density. As is expected, during the pump pulse the suprcritical surface plasma become progressively hotter as a result of thermal transport, making the plasma more reflective. This agrees with our observations. At a later time, the plasma cools gradually and its scale length in the bulk region increases, leading to increasing absorption and thus decreasing reflection of the probe light; this was seen in Fig.

1(a). From Fig. 3(b) we extract the critical density velocities and hence wavelengths shifts by Eq. (1). These shifts are then convolved over the finite probe pulse duration and shown as the solid curve in Fig. 2(a). Note that we can neglect any spectral changes due to amplitude modulation because the large frequency shifts were detected during the time interval ($-0.3 < t < 0.7$ psec) when the reflection is nearly constant as shown in Fig. 1(b). The calculated velocities show fairly good agreement with the experimental results. The discrepancy in the data at late delay $t_d \geq 0.7$ psec suggests some reduction in the rate of thermal transport. Three possible causes may be suggested: (1) The true electron thermal conductivity at the critical plasma-quartz interface region may be less than predicted by the conductivity given above. (2) The simple diffusion equation may no longer be valid for this sharp temperature gradient plasma [22], as the ratio of electron mean free path to the temperature scalelength, λ_e/L_T, is much greater than the prescribed upper limit of 2×10^{-3}. (3) At late delay times when hydrodynamic expansion becomes significant, the thermal energy of the plasma is converted into kinetic energy.

In conclusion, we have presented experimental results from both front and back side probing of a plasma produced by high intensity 100 fsec laser pulse irradiation of a transparent target. The plasma, as seen from the interior of the target, has a steep density gradient as evidenced by the reflection enhancement; and its high specular reflectivity persists for about 15 psec, much longer than the laser pulselength. In addition, comparison between the measured front and back side probe frequency shifts suggests the plasma is formed by a supersonic ionization front. These observations are thought to be manifestations of electron thermal transport phenomena. Calculations using a simplified nonlinear electron heat diffusion equation to describe evolution of plasma temperature and density show fairly good agreement with the data. And finally, the experiment has demonstrated that a solid density hot plasma can be produced, sufficiently tamped and long lived, such that other investigations should be possible, e.g., solid density plasma spectroscopy, transport properties of strongly coupled and/or Fermi degenerate plasmas.

We gratefully acknowledge A. Hazi and R. Bauer for their strong support of the project. We also wish to thank M. Eckart, R. Stewart, D. Price, and L. Van Woerkom for providing us laser time and for loan of equipment. One of us (B.-T.V.V.) acknowledges helpful discussions with R. More. This work was performed under the auspices of U.S. Department of Energy by Lawrence Livermore National Laboratory under Contract No. W-7405-ENG-48.

*Also with Department of Applied Science, University of California at Davis, Livermore, CA 94550.

[1] J. G. Fujimoto *et al.*, Phys. Rev. Lett. **53**, 1837 (1984); R. W. Schoenlein *et al.*, Phys. Rev. Lett. **58**, 1680 (1987).
[2] D. Von Der Linde, in *Resonances* (World Scientific, Singapore, 1990), p. 337; M. C. Downer *et al.*, *ibid.*, p. 324; C. V. Shank, R. Yen, and C. Hirlimann, Phys. Rev. Lett. **50**, 454 (1983).
[3] M. M. Murnane, H. C. Kapteyn, and R. C. Falcone, Phys. Rev. Lett. **62**, 155 (1989); M. M. Murnane *et al.*, Science **25**, 531 (1991).
[4] X. Y. Wang and M. C. Downer, Opt. Lett. **17**, 1450 (1992).
[5] B.-T. V. Vu, O. L. Landen, and A. Szoke, Phys. Rev. E **47**, 2768 (1993).
[6] G. J. Tallents *et al.*, Phys. Rev. A **40**, 2857 (1989).
[7] S. I. Anisimov, Sov. Phys. JETP **31**, 181 (1970).
[8] Y. B. Zeldovich and Y. P. Raizer, *Physics of Shock Waves & High Temperature Hydrodynamic Phenomena* (Academic, New York, 1966).
[9] P. Pakula and R. Sigel, Phys. Fluids **28**, 232 (1985).
[10] P. Celliers *et al.*, Phys. Rev. Lett. **68**, 2305 (1992); A. Ng *et al.*, Phys. Rev. Lett. **57**, 1595 (1986); J. A. Van Vechten, in *Semiconductors Probed by Ultrafast Laser Spectroscopy* (Academic, New York, 1984), p. 95.
[11] B.-T. V. Vu, A. Szoke, and O. L. Landen, Opt. Lett. **18**, 723 (1993).
[12] M. M. Murnane and R. W. Falcone, J. Opt. Soc. Am. B **5**, 1573 (1988).
[13] B.-T. V. Vu, Ph.D. thesis, University of California at Davis, 1993.
[14] O. L. Landen and W. E. Alley, Phys. Rev. A **46**, 5089 (1992); H. M. Milchberg and R. R. Freeman, Phys. Rev. A **41**, 2211 (1990).
[15] L. Spitzer, *Physics of Fully Ionized Gases* (Interscience, New York, 1956); M. H. Key, in *Physics of Laser Plasma*, edited by A. Rubenchik and S. Witkowski (North-Holland, Amsterdam, 1991), p. 575.
[16] Y. P. Raizer, Sov. Phys. JETP **9**, 1124 (1959).
[17] Y. T. Lee and R. M. More, Phys. Fluids **27**, 1273 (1984).
[18] J. F. Ready, J. Appl. Phys. **36**, 462 (1965).
[19] R. Fedosejevs *et al.*, Phys. Rev. Lett. **64**, 1250 (1990).
[20] H. M. Milchberg, I. Lyubomirsky, and C. G. Durfee III, Phys. Rev. Lett. **67**, 2654 (1991); H. W. K. Tom and O. R. Wood, Appl. Phys. Lett. **54**, 517 (1989).
[21] R. E. Marshak, Phys. Fluids **1**, 24 (1958).
[22] J. F. Luciani, P. Mora, and J. Virmont, Phys. Rev. Lett. **51**, 1664 (1983); E. M. Epperlein and R. W. Short, Phys. Fluids B **3**, 3092 (1991).